

# Temperature measurement of an atmospheric pressure arc discharge plasma jet using the diatomic CN ( $B^2\Sigma^+-X^2\Sigma^+$ , violet system) molecular spectra

Se Youn Moon, D. B. Kim, B. Gweon, and W. Choe<sup>a)</sup>

*Department of Physics, Korea Advanced Institute of Science and Technology, 335 Gwahangno, Yuseong-gu, Daejeon 305-701, Republic of Korea*

(Received 6 November 2008; accepted 23 January 2009; published online 11 March 2009)

The CN ( $B^2\Sigma^+-X^2\Sigma^+$ ) molecular emission spectrum is used to measure both the vibrational and rotational temperatures in atmospheric pressure arc jet discharges. The vibrational and rotational temperature effects on the synthetic diatomic molecular spectra were investigated from the  $(v',v'')=(0,0)$  band to the (5,5) band. The temperatures obtained from the synthetic spectra compared with the experimental result of a low-frequency arc discharge show a vibrational temperature of (4250–5010) K and a rotational temperature of (3760–3980) K for the input power in the range of (80–280) W. As the (0,0) band is isolated from other vibrational transition bands, determination of the rotational temperature is possible based only on the (0,0) band, which simplifies the temperature measurement. From the result, it was found that the CN molecular spectrum can be used as a thermometer for atmospheric pressure plasmas containing carbon and nitrogen. © 2009 American Institute of Physics. [DOI: 10.1063/1.3087537]

## I. INTRODUCTION

Optical emission spectroscopy is a powerful noninvasive diagnostic method for plasmas. Spectroscopic methods are frequently favored especially for atmospheric pressure plasmas, as conventional diagnostics such as electrostatic probes are generally less useful due to the very frequent collisions that occur among particles under a high gas pressure.<sup>1,2</sup> The spectrum emitted from the plasma gives important information such as identification of existing species (atoms, molecules, and radicals), as well as the temperatures and electron density through spectrum analyses.<sup>3</sup> Among these parameters, the plasma temperatures, such as the vibrational temperature and rotational temperature, provide knowledge of the chemical reactivity of the molecules existing in the plasmas. The vibrational temperature ( $T_{\text{vib}}$ ) is related to the energy transfer between electrons and heavy particles, especially molecules. In general,  $T_{\text{vib}}$  lies between the gas temperature and the electron temperature and shows a tendency similar to that of the electron temperature.<sup>3,4</sup> On the other hand, as the rotational temperature ( $T_{\text{rot}}$ ) is related to collisions among heavy particles such as neutrals and molecules, measurement of  $T_{\text{rot}}$  is important to estimate the neutral temperature or gas temperature of the plasma. The gas temperature, which is defined as the kinetic temperature of heavy particles, can be obtained by measuring the rotational temperature of the diatomic molecular spectra in atmospheric pressure plasmas because the rotational-translational relaxation occurs quickly enough to equilibrate the rotational temperature and the gas temperature.<sup>5,6</sup>

If an atmospheric pressure plasma is generated in the ambient air, OH or  $N_2^+$  diatomic molecules can be used to

measure the temperature since the emissions from the rotational states of the molecules are easily observed due to air and/or water impurities.<sup>1,2,5</sup> However, given that the vibrational spectral bands do not easily appear in their radicals, measurement of the vibrational temperature using the vibrational spectra is not easy. For example, the spectral intensities emitted from the higher vibrational states of OH are very small compared to the intensity of the (0-0) vibrational state.<sup>7</sup> In addition, because the molecular emission spectra of widely used gases in plasma processing such as carbon or methane are blended with the spectra of OH or  $N_2^+$  molecules, temperature measurements using those spectra are somewhat complicated. On the other hand, the CN spectrum is found in many extraterrestrial sources such as the Sun, the stellar atmosphere, comets, and various plasma sources such as arcs, flames, shock tube, and electrical discharges generated for environmental and material applications.<sup>7-9</sup> The violet system ( $B^2\Sigma^+-X^2\Sigma^+$ ) is the most easily observed, and the red system ( $A^2\Pi-X^2\Sigma^+$ ) in the near infrared range is also a strong and important band.<sup>7</sup> In addition, the CN spectrum is easily observed in methane ( $CH_4$ ) based plasmas containing nitrogen and/or hydrogen of the type that are generally used for the production of amorphous carbon nitride films, in the deposition of diamondlike carbon films, for the modification of material surfaces into superhydrophobic surfaces, in gas reformation processes, and for plasma-enhanced combustion.<sup>10-12</sup> In this work, the CN ( $B^2\Sigma^+-X^2\Sigma^+$ , violet system) emission spectrum is used to measure the temperature of an atmospheric pressure methane-aided arc discharge. From an application point of view, accurate measurement of both  $T_{\text{rot}}$  and  $T_{\text{vib}}$  is crucial in the optimization and control of the application performance, as the plasma temperatures play a main role in plasma processes.

<sup>a)</sup> Author to whom correspondence should be addressed. Electronic mail: wchoe@kaist.ac.kr

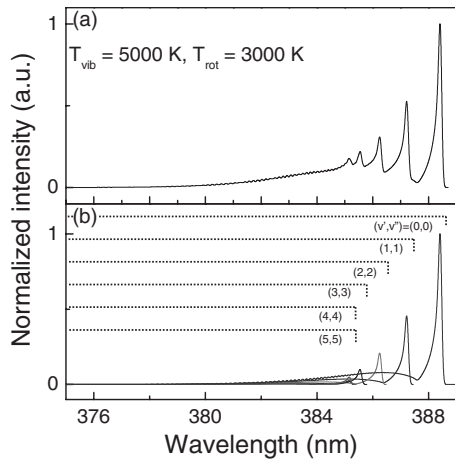


FIG. 1. (a) The synthetic CN (violet system) spectrum at  $T_{\text{vib}}=5000$  K,  $T_{\text{rot}}=3000$  K, and  $\Delta_i=0.10$  nm. (b) Each rotational band for each vibrational state from (0,0) to (5,5).

## II. MOLECULAR SPECTRA OF CN ( $B^2\Sigma^+-X^2\Sigma^+$ , VIOLET SYSTEM)

The emission intensity of the CN band,  $I_{\nu', \nu'', J', J''}$ , as a function of both  $T_{\text{rot}}$  and  $T_{\text{vib}}$  is given by<sup>4,13</sup>

$$I_{\nu', \nu'', J', J''} \propto q_{\nu', \nu''} S_{J', J''} (\nu_{J', J''})^4 \exp\left(-\frac{F_{J'} hc}{kT_{\text{rot}}}\right) \exp\left(-\frac{G_{\nu'} hc}{kT_{\text{vib}}}\right), \quad (1)$$

where  $q_{\nu', \nu''}$  is the Franck–Condon factor,  $S_{J', J''}$  denotes the rotational band strengths,  $\nu_{J', J''}$  is the emission light frequency,  $h$  is the Planck constant,  $c$  is the speed of light, and  $k$  is the Boltzmann constant. The subscripts  $J'$ ,  $J''$  and  $\nu'$ ,  $\nu''$  are the upper and the lower states of rotational and vibrational transitions, respectively, and  $F_{J'}$  and  $G_{\nu'}$  are the rotational and the vibrational terms of the excited states in  $\text{cm}^{-1}$ , respectively. For an accurate measurement of both  $T_{\text{rot}}$  and  $T_{\text{vib}}$  out of the measured emission intensities, however, the dependence of each temperature and line broadening effect on the spectrum shape should be considered first. Generally, an experimentally obtained emission intensity profile appears as a convolution of various broadenings including instrumental, Doppler, and Stark broadening. Since the instrumental broadening in our experimental arrangement was dominant compared to others and was found to have a Gaussian shape, the intensity profile becomes the convolution of Eq. (1) and a Gaussian function with a full width at half maximum,  $\Delta_i$ .<sup>1</sup>

A typical CN violet synthetic spectrum using Eq. (1) at  $T_{\text{vib}}=5000$  K and  $T_{\text{rot}}=3000$  K with appropriate constants by Herzberg<sup>4</sup> is presented in Fig. 1(a). The most prominent band is that of the  $(\nu', \nu'')=(0,0)$  of  $\Delta v=0$  transition, which overlaps with other  $\Delta v=0$  transition bands from  $(\nu', \nu'')=(1,1)$  to (5,5). The bands were selected due to their available strengths, as shown in Fig. 1(b). The synthetic spectra of CN for various  $T_{\text{vib}}$ ,  $T_{\text{rot}}$ , and  $\Delta_i$  values are depicted in Fig. 2, in which each spectrum is normalized with respect to the (0,0) transition band head for the sake of simplicity. Increasing  $T_{\text{rot}}$  at the same value of  $T_{\text{vib}}$  results in a decrease in the intensities of each vibrational transition with respect to the (0,0) band head, but each vibrational band head is more clearly

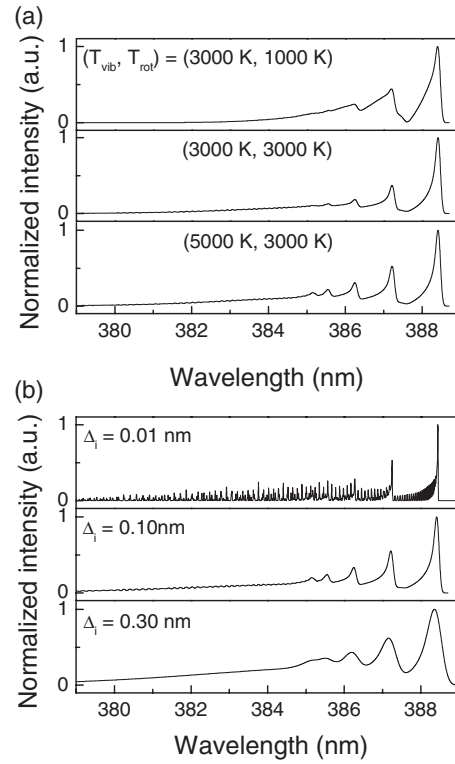


FIG. 2. (a) The synthetic CN (violet system) spectra at various  $T_{\text{vib}}$  and  $T_{\text{rot}}$  at fixed  $\Delta_i=0.1$  nm. (b) The synthetic CN (violet system) spectra at different  $\Delta_i$  from 0.01 to 0.30 nm ( $T_{\text{vib}}=T_{\text{rot}}=5000$  K).

appeared. On the other hand, increasing  $T_{\text{vib}}$  at the same value of  $T_{\text{rot}}$  makes each vibrational band head clearer and changes the relative intensity ratios of the bands. In addition, a larger  $\Delta_i$  brings about a larger width of the rotational spectra in each vibrational transition, as depicted in Fig. 2(b).

The dependence of  $T_{\text{vib}}$  on the intensities of the vibrational band heads and the isolation among their vibrational states makes the measurement of  $T_{\text{vib}}$  possible using the Boltzmann plot method.<sup>4</sup> In doing so, the effects of both  $T_{\text{rot}}$  and  $\Delta_i$  should be simultaneously taken into account. Figure 3 presents the Boltzmann plots as obtained from the simulated spectra [Eq. (1)] with different values of  $T_{\text{rot}}$  and  $\Delta_i$ . For comparison, the straight lines in the figure represent cases that take  $T_{\text{vib}}$  into account so that the line slopes  $1/kT_{\text{vib}}$  indicate the given vibrational temperature  $T_{\text{vib}}=5000$  K. On the other hand, by taking  $T_{\text{rot}}$  as well as  $\Delta_i=0.1$  nm into account, the shape of the Boltzmann plot, especially in the large vibrational number regime, changes significantly as shown in Fig. 3(a). It is because the rotational spectrum of (0,0) band seriously influences other band spectra depicted in Fig. 1(b). In the same manner, the line slope is decreased and distorted from a straight line to a curved shape as  $\Delta_i$  is increased from 0.01 to 0.30 nm [Fig. 3(b)]. This suggests that a high spectral resolution spectrometer is needed. Therefore, significant error can occur during the determination of  $T_{\text{vib}}$  using the Boltzmann plots of the CN spectra without simultaneously considering both  $T_{\text{rot}}$  and  $\Delta_i$  concurrently.

Another way of measuring the temperatures is by fitting the synthetic spectra to the measured spectra. When the contributions from both temperatures to the spectrum shape are large, as in the CN spectra, this process is usually time con-

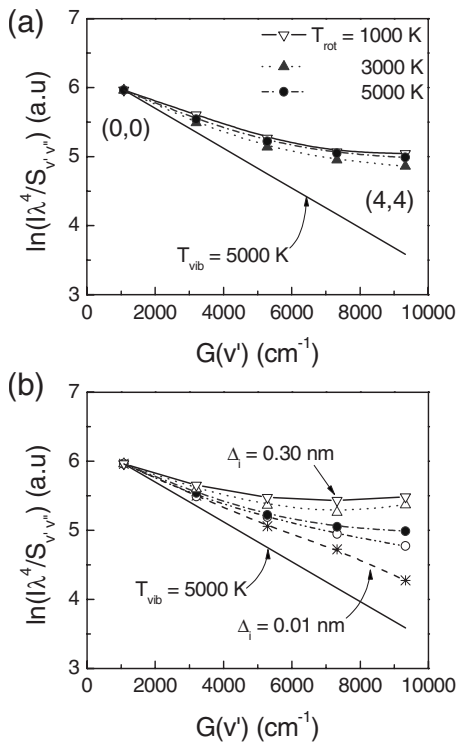


FIG. 3. (a) Difference in the Boltzmann plot caused by different  $T_{rot}$  values ( $T_{vib}=5000$  K (—) and  $\Delta_i=0.01$  nm). (b) Difference in the Boltzmann plot due to different  $\Delta_i$  values:  $\Delta_i=0.01$  nm (—\*),  $0.05$  nm (—○—),  $0.10$  nm (—●—),  $0.20$  nm (—△—), and  $0.30$  nm (—▽—). The straight line indicates the Boltzmann plot for  $T_{vib}=5000$  K without considering the instrumental broadening.

suming and less accurate. In the following section, a simpler method of “separately” determining  $T_{rot}$  and  $T_{vib}$  using the CN (0,0) band from 387 to 389 nm is demonstrated.

### III. SEPARATE MEASUREMENT $T_{ROT}$ AND $T_{VIB}$

The CN spectra were observed in the atmospheric pressure arc discharge plasma produced in ambient air in the set up illustrated in Fig. 4(a). The plasma source consisted of a 20 kHz ac power supply, a powered rod electrode surrounded by a cylindrical dielectric tube for gas injection, and a grounded electrode with a 2 mm hole. The distance between the two electrodes was 15 mm. A mixed gas,  $CH_4$  of 2.6 SLM, SLM denotes standard liters per minutes,  $O_2$  of 2.5 SLM, and  $N_2$  of 5.6 SLM, was injected to generate the plasmas. As clearly depicted in the plasma image, the discharge showed two distinctive regions of its arc and jet. Electrical measurements were performed using voltage (Tektronix P6015A) and current (Tektronix TCP303, TCPA300 amplifier) probes. Figure 4(b) illustrates a current-voltage oscillogram during the discharge, of which the phase angle between the current and voltage is nearly zero due to the high conductivity of the arc discharge. During a half period, more than four successive discharges were observed in the current and voltage signals, and they were also visually confirmed by random arc generations in the arc region. The emission spectra were obtained using a spectrometer (Acton SpectraPro 500i: 500 mm focal length, 1200 grooves/mm grating, and 300 nm blaze wavelength) with a charge coupled device (CCD) (Princeton Instrument) detector in the

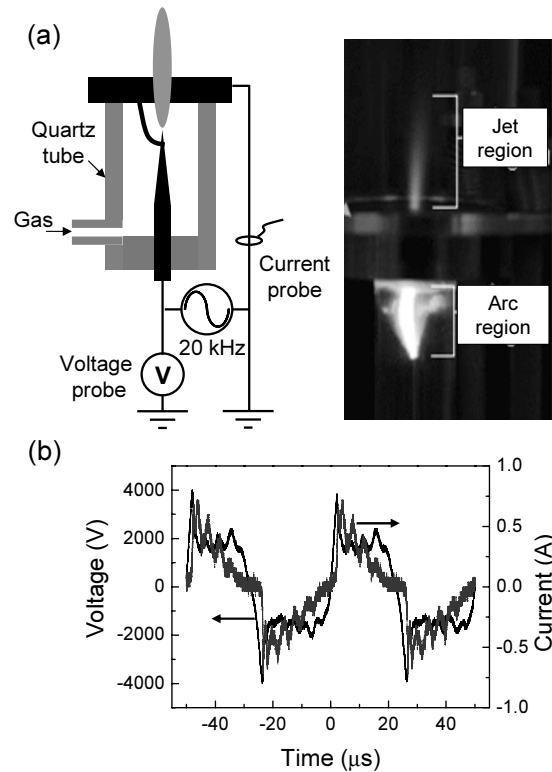


FIG. 4. Schematic illustration of the (a) experimental setup for atmospheric pressure arc discharge, and (b) voltage and current oscillogram during the discharge.

jet region where the optical plasma emission was spatially stable and temporally continuous. Depending on the experimental conditions, the entrance slit width and the CCD integration times varied from 10 to 30  $\mu\text{m}$  and from 15 to 50 ms, respectively.

Figure 5 depicts a typical emission spectrum obtained from the jet region from 300 to 440 nm at various input powers of 80, 180, and 280 W. Due to the injected gases and air impurities, the CN (violet system),  $N_2$  (second positive system), and OH (306.4 nm system) molecular spectra can be observed. Raising the input power increases the line-integrated emission intensities of the visible range. In addition, Cu I lines (324.8 and 327.4 nm) also appear at a high input power due to the evaporation of the copper electrode.<sup>14</sup>

In this work, both  $T_{rot}$  and  $T_{vib}$  were obtained by com-

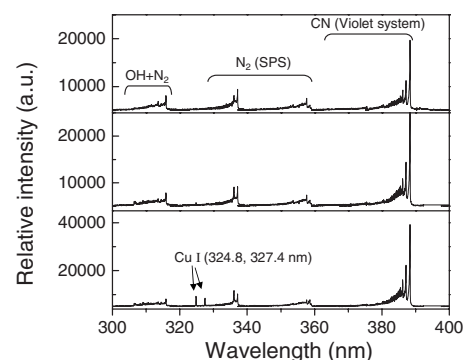


FIG. 5. Emission spectra at various input power: 80, 180, and 280 W. Due to the mixed gas of  $CH_4$ ,  $N_2$ , and  $O_2$ , and air impurities, the OH,  $N_2$ , and CN molecular spectra are observed.

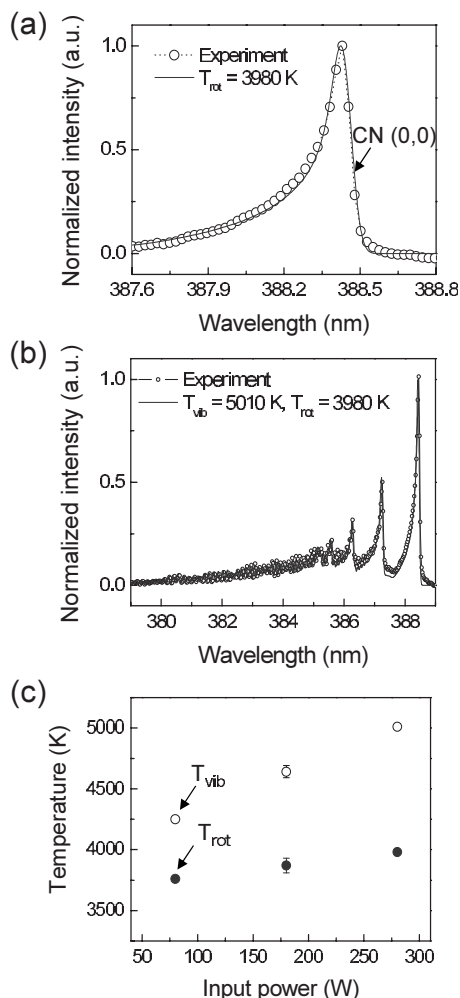


FIG. 6. (a)  $T_{rot}$  obtained by the comparison between the experimental result (—○—) and the synthetic spectrum (—) of CN (0,0) band is 3980 K. (b) Comparison of the whole CN spectra provides  $T_{vib}$  of 5010 K and  $T_{rot}$  of 3980 K at 280 W. (c) As the input power is increased, both  $T_{vib}$  and  $T_{rot}$  are also increased from 4250 to 5010 K and from 3760 to 3980 K, respectively.  $\Delta\lambda=0.065$  nm.

paring the experimental spectra and the synthetic spectra of the CN band through a chi-square fitting. Both temperatures can be obtained by selecting the values which produce the best fit when using both  $T_{rot}$  and  $T_{vib}$  as fitting parameters. It is noted that, in this work,  $T_{rot}$  is obtained based solely on the CN (0,0) band in the (387–389) nm range since it is pretty much isolated from other transition bands, as shown in Fig. 1(b). Figure 6(a) depicts a comparison of the experimentally obtained CN (0,0) band (—○—) and the synthetic rotational spectrum (—), producing  $T_{rot}$  of 3980 K. Upon knowing the  $T_{rot}$  value,  $T_{vib}$  is obtained by using the entire CN band spectrum, as shown in Fig. 6(b), where  $T_{vib}=5010$  K.

Finally, Fig. 6(c) describes the dependence of the temperatures on the input power. As the input power is increased, both  $T_{vib}$  and  $T_{rot}$  increased from 4250 to 5010 K

and from 3760 to 3980 K, respectively, as expected. As the jet plasma region is not an active region for the plasma generation and the plasma is cooled down by the surroundings,  $T_{vib}$  and  $T_{rot}$  are not in the local thermodynamic equilibrium state.

#### IV. SUMMARY

Using the CN molecular spectrum (violet system) emitted from an atmospheric pressure arc discharge, the vibrational and rotational temperatures were evaluated. In the CN spectrum, since the rotational temperature and the degree of line broadening significantly influence the spectrum shape, employment of the typical Boltzmann plot method is limited for accurate  $T_{vib}$  measurements. Therefore, the synthetic method considering both temperatures and the instrumental line broadening was used. In addition, the independent measurement of  $T_{rot}$  using the CN (0,0) band from 387 to 389 nm rather than the simultaneous determination of both  $T_{rot}$  and  $T_{vib}$  using the entire CN spectrum makes the measurement relatively simpler and quicker. Applying the proposed method in an atmospheric arc discharge using  $\text{CH}_4/\text{O}_2/\text{N}_2$  mixed gases was attempted. In the (80–280) W input power range,  $T_{vib}=(4250\text{--}5010)$  K and  $T_{rot}=(3760\text{--}3980)$  K. This diagnostic method will be useful to plasmas using  $\text{CH}_4$  based discharges containing carbon/nitrogen in many industrial applications without a great deal of consideration of the spectral resolution, as in the Boltzmann plot.

#### ACKNOWLEDGMENTS

This work was partly supported by Korea Institute of Machinery and Materials. The authors thank to Dr. Y. H. Song, Dr. M. S. Cha, Dr. D. H. Lee, and Ms. N. K. Hwang for their technical supports and discussions.

- <sup>1</sup>S. Y. Moon and W. Choe, *Spectrochim. Acta, Part B* **58**, 249 (2003).
- <sup>2</sup>O. Motret, C. Hibert, S. Pellerin, and J. M. Pouvesle, *J. Phys. D: Appl. Phys.* **33**, 1493 (2000).
- <sup>3</sup>W. Lochte-Holtgreven, *Plasma Diagnostics* (AIP, New York, 1968).
- <sup>4</sup>G. Herzberg, *Molecular Spectra and Molecular Structure I. Spectra of Diatomic Molecules*, 2nd ed. (Van Nostrand, Princeton, 1964).
- <sup>5</sup>S. Pellerin, J. M. Cormier, F. Richard, K. Musiol, and J. Chapelle, *J. Phys. D: Appl. Phys.* **29**, 726 (1996).
- <sup>6</sup>A. Czernichowski, *J. Phys. D: Appl. Phys.* **20**, 559 (1987).
- <sup>7</sup>R. W. B. Pearse and A. G. Gaydon, *The Identification of Molecular Spectra* (Chapman and Hall, London, 1976).
- <sup>8</sup>D. L. Lambert, J. A. Brown, K. H. Hinkle, and H. R. Johnson, *Astrophys. J.* **284**, 223 (1984).
- <sup>9</sup>G. Fedosenko, J. Engemann, and D. Korzec, *Surf. Coat. Technol.* **133–134**, 535 (2000).
- <sup>10</sup>J. H. Kim, D. H. Ahn, Y. H. Kim, and H. K. Baik, *J. Appl. Phys.* **82**, 658 (1997).
- <sup>11</sup>V. R. Axel, L. Serge, M. Philippe, and S. Vladmir, *Plasma Sources Sci. Technol.* **16**, 149 (2007).
- <sup>12</sup>S. C. Cho, Y. H. Hong, and H. S. Uhm, *J. Mater. Chem.* **17**, 232 (2007).
- <sup>13</sup>S. Acquaviva, *Spectrochim. Acta, Part A* **60**, 2079 (2004).
- <sup>14</sup>A. Risacher, S. Larigaldie, G. Bobillot, J.-P. Marcellin, and L. Picard, *Plasma Sources Sci. Technol.* **16**, 200 (2007).